University of Reading

Diacenaphthylene-fused benzo[1,2-b:4,5-b']dithiophenes: polycyclic heteroacenes containing full-carbon five-membered aromatic rings

Article

Accepted Version

Wu, H., Fang, R., Tao, J., Wang, D., Qiao, X., Yang, X., Hartl, F. ORCID: https://orcid.org/0000-0002-7013-5360 and Li, H. (2017) Diacenaphthylene-fused benzo[1,2-b:4,5-b']dithiophenes: polycyclic heteroacenes containing full-carbon five-membered aromatic rings. Chemical Communications, 53 (4). pp. 751-754. ISSN 1364-548X doi: 10.1039/C6CC09184A Available at https://centaur.reading.ac.uk/68369/

It is advisable to refer to the publisher's version if you intend to cite from the work. See Guidance on citing.

To link to this article DOI: http://dx.doi.org/10.1039/C6CC09184A

Publisher: The Royal Society of Chemistry

All outputs in CentAUR are protected by Intellectual Property Rights law, including copyright law. Copyright and IPR is retained by the creators or other copyright holders. Terms and conditions for use of this material are defined in the End User Agreement.

University of Reading

www.reading.ac.uk/centaur

CentAUR

Central Archive at the University of Reading

Reading's research outputs online

CrossMark
click for updates

View Article Online
View Journal

ChemComm

Accepted Manuscript

This article can be cited before page numbers have been issued, to do this please use: H. Wu, R. Fang, J. Tao, D. Wu, X. Qiao, X. Yang, F. Hartl and H. Li, *Chem. Commun.*, 2016, DOI: 10.1039/C6CC09184A.

This is an Accepted Manuscript, which has been through the Royal Society of Chemistry peer review process and has been accepted for publication.

Accepted Manuscripts are published online shortly after acceptance, before technical editing, formatting and proof reading. Using this free service, authors can make their results available to the community, in citable form, before we publish the edited article. We will replace this Accepted Manuscript with the edited and formatted Advance Article as soon as it is available.

You can find more information about Accepted Manuscripts in the author guidelines.

Please note that technical editing may introduce minor changes to the text and/or graphics, which may alter content. The journal's standard Terms & Conditions and the ethical guidelines, outlined in our author and reviewer resource centre, still apply. In no event shall the Royal Society of Chemistry be held responsible for any errors or omissions in this Accepted Manuscript or any consequences arising from the use of any information it contains.

ROYAL SOCIETY OF CHEMISTRY

rsc.li/chemcomm

Please do not adjust margins

View Article Online
DOI: 10.1039/C6CC09184A

Journal Name

COMMUNICATION

Diacenaphthylene-Fused Benzo[1,2-b:4,5-b']dithiophenes: Polycyclic Heteroacenes Containing Full-Carbon Five-Membered Aromatic Rings

Received 00th January 20xx,
Accepted 00th January 20xx

DOI: 10.1039/x0xx00000x

www.rsc.org/

Hongzhuo Wu [a], Renren Fang [a], Jingwei Tao [a], Deliang Wang [a], Xiaolan Qiao [a], Xiaodi Yang [c,] *, František Hartl [b,] *, Hongxiang Li [a,] *

We herein report on an efficient synthesis of diacenaphthylene-fused benzo[1,2-b:4,5-b']dithiphenes and demonstrate that their packing structure in the solid state depends on the substituent groups. These compounds form dimers with their radical cations in high solution concentration and display good field-effect mobility.

Polycyclic aromatic compounds (PACs) are of great interest because of their unique electronic structures and physical properties, and wide applications as functional materials.[1-4] PACs are usually composed of six-membered benzene rings and/or five-membered heteroaromatic rings (such as thiophene, pyrrole and furan).[5-7] A full-carbon five-membered aromatic ring is an analogue of five-membered heteroaromatic rings and a building block of fullerenes. Recently, planar cyclopenta-fused polycyclic arenes (such as acenaphthylenes, dibenzopentalenes and indenofluorenes) featuring full-carbon five-membered *anti-aromatic* rings, have intensely been investigated.[11-15] However, planar PACs containing full-carbon five-membered *aromatic* rings (FC-PACs) are rarely reported, even though some of them display special self-assembly properties, good transistor and solar cell performance, and biradical characteristics.[8-12] Hence it is of great importance and general interest to synthesize new type of FC-PACs and explore their fundamental properties as well as practical applications. Currently, the synthetic strategies to FC-PACs are limited and remain challenging, usually involving tedious synthetic steps and/or poor reaction scope. Herein, with Pd-catalyzed C–H activation reaction, we report on a facile synthesis of nine-ring fused planar FC-PACs, diacenaphthylene fused benzo[1,2-b:4,5-b']dithiophenes **M2-M6** (Scheme 1).

There has been a growing interest in dimerization of π-conjugated molecules and their radical cations studied with a dual purpose, viz. (i) understanding the nature of the charge-transport phenomena in p-doped organic semiconductors, and (ii) potential application of these compounds in material science and supramolecular chemistry, such as switches, molecular motors, data storage systems and so on.[16-18] Interestingly, planar rigid FC-PACs **M2-M6** display rich redox behavior and form dimers with their radical cations at high solution concentration, being confirmed with solution dependent differential pulse voltammogram (DPV) and spectroelectrochemistry. The application of CF-PACs as semiconductors in transistors was also investigated.

Table 1. Pd-catalyzed C–H activation reaction of benzo[b]thiophene with 1,8-dibromonaphthalene.

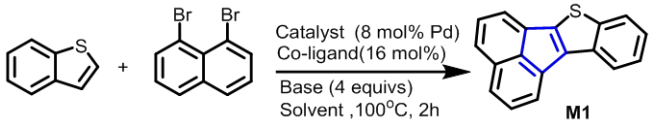

Entry	Catalyst	Co-ligand	Base	Solvent	Yield [a]
1	$Pd(OAc)_2$	$P(t\text{-}Bu)_2Me{\cdot}HBF_4$	KOAc	DMA	35.7%
2	$Pd(OAc)_2$	$P(t\text{-}Bu)_2Me{\cdot}HBF_4$	K_2CO_3	DMA	68.7%
3	$Pd(OAc)_2$	$P(t\text{-}Bu)_2Me{\cdot}HBF_4$	Cs_2CO_3	DMA	11.9%
4	$Pd_2(dba)_3$	$P(t\text{-}Bu)_2Me{\cdot}HBF_4$	KOAc	DMA	30.1%
5	$Pd(PPh_3)_2Cl_2$	$P(t\text{-}Bu)_2Me{\cdot}HBF_4$	KOAc	DMA	30.1%
6	$Pd(OAc)_2$	$P(t\text{-}Bu)_2Me{\cdot}HBF_4$	KOAc	toluene	0
7	$Pd(OAc)_2$	$P(t\text{-}Bu)_2Me{\cdot}HBF_4$	KOAc	dioxane	0
8	$Pd(OAc)_2$	$P(Cy)_3.HBF_4$	KOAc	DMA	7.1%
9	$Pd(OAc)_2$	$P(o\text{-}tolyl)_3$	KOAc	DMA	6.3%

[a] Yield of isolated product

To explore the application of catalyzed C–H activation reactions for the syntheses of CF-PACs, benzo[*b*]thiophene and 1,8-dibromonaphthalene were first used as model substrates (Table 1). The co-ligand, base and solvent were found to strongly affect the reaction yield; the optimum conditions were using $Pd(OAc)_2$ as the catalyst, $P(t\text{-}Bu)_2Me{\cdot}HBF_4$ as the co-ligand and K_2CO_3 as the base in DMA at 100°C (Table 1,

[a] Shanghai Institute of Organic Chemistry, Chinese Academy of Sciences, Shanghai, 200032, China. E-mail: lhx@mail.sioc.ac.cn
[b] Department of Chemistry, University of Reading, Whiteknights, Reading RG6 6AD, United Kingdom. E-mail: f.hartl@reading.ac.uk
[c] Laboratory of Advanced Materials, Fudan Univeristy, Shanghai, 200438, China. E-mail: yangxiaodi@fudan.edu.cn
Electronic Supplementary Information (ESI) available: [Synthetic procedure and compound characterizations, electrochemistry result, single crystal CIF files]. See DOI: 10.1039/x0xx00000x

Published on 08 December 2016. Downloaded by University of Reading on 09/12/2016 09:02:42.

ChemComm Accepted Manuscript

Please do not adjust margins

Published on 08 December 2016. Downloaded by University of Reading on 09/12/2016 09:02:42.

entry 2). When benzo[*b*]thiophene was replaced by the larger conjugated benzo[1,2-*b*:4,5-*b'*]-dithiophene derivatives, the common organic semiconductor building blocks, nine-ring fused CF-PACs **M2-M4** with two aromatic full-carbon five-membered rings were synthesized in a one-pot step (Scheme 1).[19] By changing the alkyl chains to more electron-donating alkoxy chains, the reactions worked well. When electron-deficient benzo[1,2-*b*:4,5-*b'*]dithiophene-4,8-dione was reacted with 1,8-dibromonaphthalene under the above conditions, compound **M5** was obtained as an insoluble gray powder in 90% yield. Compound **M5** further reacted with 5-ethynyl-1,3-di(*t*-butyl)benzene, having afforded soluble and larger π-conjugated compound **M6**. The above results demonstrate the successful applications of a C–H activation reaction in the preparation of CF-PACs.

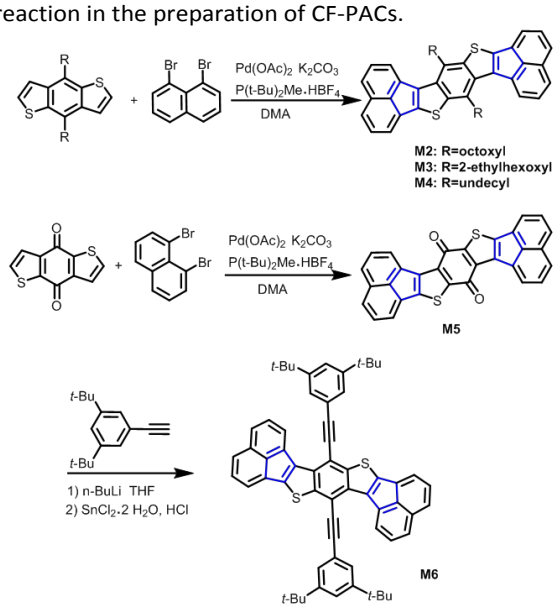

Scheme 1. Syntheses and chemical structures of CF-PACs **M2-M6.**

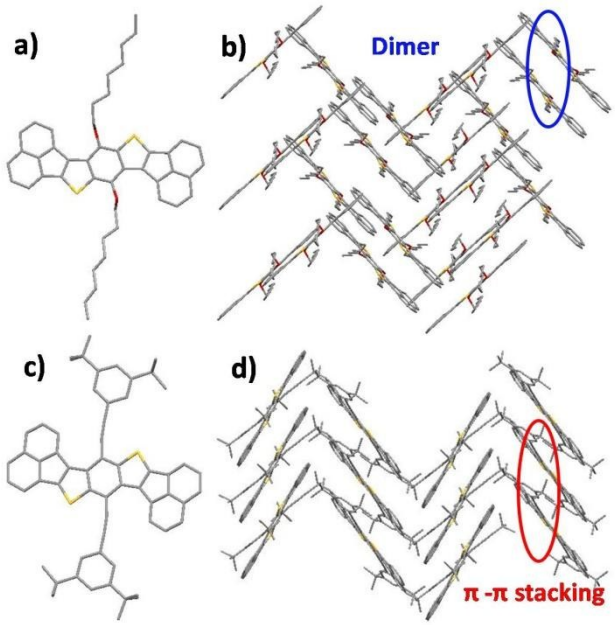

Figure 1. Crystal and packing structures of **M2** (a-b) and **M6** (c-d).

Single crystals of **M2** and **M6** were grown from dichloromethane / hexane using the solvent evaporation method (Figure 1). The XRD data show that **M2** belongs to a triclinic space group P-1, with the cell parameters a = 13.0940(7) Å, b = 14.5388(8) Å, c = 20.6868(12) Å, α= 76.383(2)°, β= 82.5890(10)° and γ = 80.352(2)°. In the single crystal, the conjugated core exhibits a planar structure, and the side chains are positioned out of the plane. Molecules of **M2** form dimers in the crystals. Strong π-π interactions with an interplane distance of 3.459 Å and hydrogen bonds between O of the alkoxy substituent and H of the alkyl chain are observed in the dimers. C–H…π interactions are encountered between the dimers. Similar to **M2**, the conjugated core of **M6** shows a planar structure and the phenyl ring of the phenylacetylene substituent is out of the plane. However, the packing structure of **M6** is different from that of **M2**. The single crystals of **M6** belong to a monoclinic space group C2/c, with the cell parameters a = 41.379(8) Å, b = 6.0824(12) Å, c = 20.059(4) Å and β = 106.27(3)°. **M6** adopts a typical herringbone structure in the crystal, and slipped π-π stacking with a distance of 3.426 Å is observed. Moreover, C–H…π interactions between the conjugated cores exist for adjacent π-π stackings. Unlike **M2**, the slipped π-π stacking structure of **M6** facilitates charge carrier transport and suggests its potential application as a semiconductor in organic transistors.

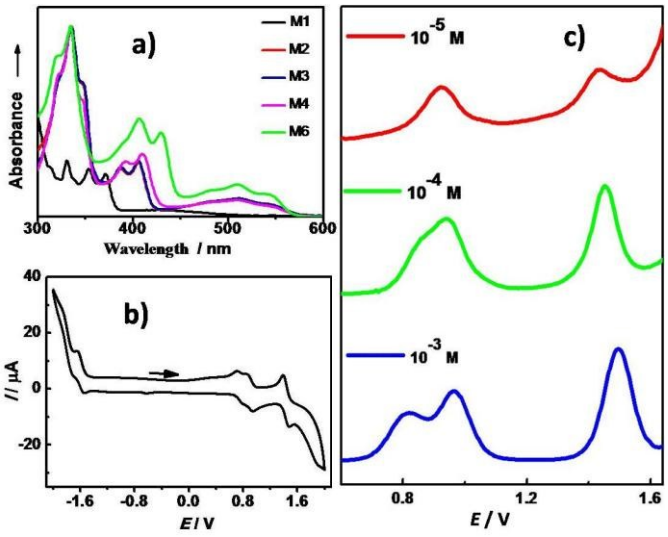

Figure 2. a) UV-vis absorption spectra of **M1**-**M4** and **M6** in CH_2Cl_2. b) Cyclic voltammogram (CV) of **M4** (10^{-3} M). c) Differential pulse voltammograms (DPV) of **M4** at different concentrations. The CVs and DPVs were measured in CH_2Cl_2 solutions, using 10^{-1} M *n*-Bu_4PF_6 as the supporting electrolyte, and SCE as the reference at the scan rate v = 100 mV s^{-1}.

The electronic absorption spectra of **M1**-**M4** and **M6** in CH_2Cl_2 are shown in Figure 2a. All compounds absorb in the range of 300 - 600 nm. Compared to **M1**, the onset of the low-lying structured absorption bands of **M2**-**M6** is strongly bathochromically shifted by ca 4500 cm^{-1} (0.55 eV), which nicely agrees with the smaller HOMO-LUMO gap determined by cyclic voltammetry (Figure 2b and Figure S2, Supporting Information), see below. This difference is ascribed to the increased conjugation length of **M2-M4** and **M6** that have very

View Article Online DOI: 10.1039/C6CC09184A

ChemComm Accepted Manuscript

This journal is © The Royal Society of Chemistry 20xx

Published on 08 December 2016. Downloaded by University of Reading on 09/12/2016 09:02:42.

View Article Online
DOI: 10.1039/C6CC09184A

similar electronic absorption spectra, with two vibronically structured absorption bands at ca 400 and 500 nm. The former absorptions are slightly red-shifted in the order of alkyl <alkoxy< phenylacetylene, likely because of the increased electron-donating nature of the substituents and the enlarged conjugation structures.

The redox properties of **M1**-**M4** and **M6** were first investigated by cyclic voltammetry (CV) in dichloromethane (Figure 2b and Figure S2 in Supporting Information). **M1** displays in the available potential window only one reversible electron oxidation and one reversible reduction near the electrolyte limits. Both processes exhibit similar peak currents, in line with their reversible nature. Interestingly, **M2**-**M4** and **M6** show richer redox chemistry, with two cathodic and three anodic steps observable at the concentration of 10^{-3} M. Importantly, the first two anodic steps are closely spaced and their peak currents reach *ca.* one half of the peak currents for the first cathodic wave and the third anodic wave. The corresponding DPV measurements with **M4**, selected for a detailed study**,** have shown that the first and second anodic waves fuse gradually with decreasing the concentration of the compound. For 10^{-5} M **M4**, only two anodic peaks with equal current intensities are observed at room temperature (Figure 2b). This concentration dependence indicates the formation of dimers between **M4** and its radical cation, $[\mathbf{M4}–\mathbf{M4}]^{+}$, at sufficiently high concentrations.[18,20] This explanation is supported by the dominant localization of the initial anodic step on the central benzodithiophene part (Figure S1, Supporting Information – the unsubstituted model of **M4**). The oxidation potential of the non-oxidized half of the cationic dimer then becomes slightly positively shifted. Apparently, doubly oxidized dimer $[\mathbf{M4}–\mathbf{M4}]^{2+}$ is unstable at ambient temperature and dissociates to $[\mathbf{M4}]^{+}$ radicals further oxidizing to $[\mathbf{M4}]^{2+}$ at the electrode potential of the third, one-electron anodic wave. More support for this peculiar anodic behavior of **M4** is given in the following spectroelectrochemical section.The redox potentials of **M1**-**M4** and **M6** are summarized in Table S1. **M2**-**M4** and **M6** have their HOMO-LUMO band gap larger than 2.3 eV and the HOMO energy levels at about 5.10 - 5.40 eV, suggesting their application as organic semiconductors in p-type organic transistors.

The redox behavior of undecyl-substituted compound **M4**, selected to represent the whole series, was monitored by *in situ* UV-vis-NIR spectroelectrochemistry (Figure 3; saturated solution in dichloromethane) in combination with thin-layer cyclic voltammetry within an OTTLE cell to confirm the stability of the redox products.[21] The reversible reduction of **M4** to $[\mathbf{M4}]^{-}$ is accompanied by the growth of a broad absorption band at 720 nm. The spectral changes accompanying the oxidation of **M4** to $[\mathbf{M4}]^{+}$ reveal that this process occurs in two separate steps, in accordance with the CV and DPV scans (Figure 2). Initially (at 0.7 V), the intense sharp parent absorption at 320 nm drops to ca one half of the total absorbance and new absorption bands grow at 750 and 1000 nm. The bifurcated parent absorption at 400 nm is still apparent in the resulting spectrum. Moving the anodic potential to the second anodic wave at 0.8 V causes further

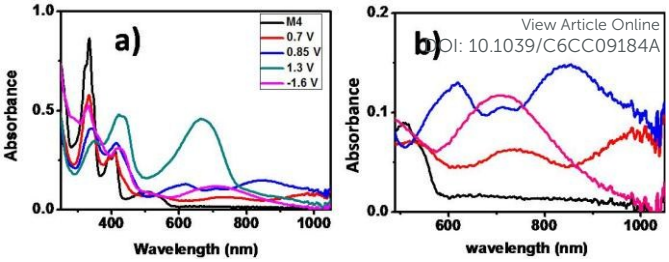

Figure 3. (a) The electronic absorption spectra of neutral **M4** (black curve) in dichloromethane (the saturated solution at 293 K) and its stable charged redox forms, viz. $[\mathbf{M4}]^{-}$ (purple curve), dimer $[\mathbf{M4}\text{-}\mathbf{M4}]^{+}$(red curve), $[\mathbf{M4}]^{+}$ (blue curve) and $[\mathbf{M}]^{2+}$ (turquoise curve). (b)The zoomed out spectral range of 500-1100 nm.

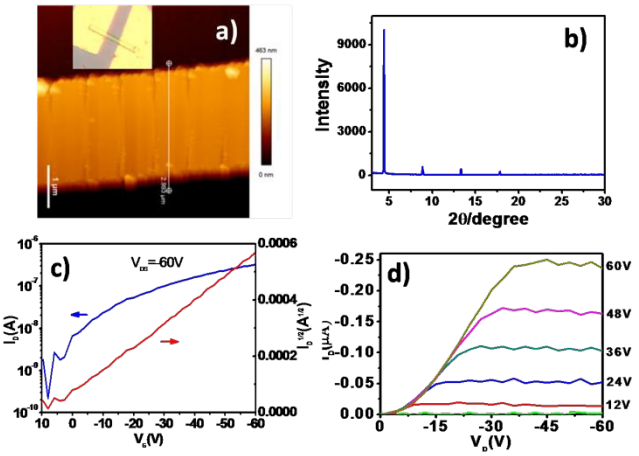

Figure 4. a) AFM image of the micro-/nano-sized wires of **M6** deposited on the OTS-modified Si/SiO_2 substrates; (insert) the optical image of a micro-sized wire transistor. b) XRD patterns of the micro-sized wires. c)-d) The transfer and output curves of **M6** based microwire transistors.

decrease of the parent absorption at 320 nm and the bifurcated band at 400 disappears. In the visible-NIR region, however, new absorption bands grow at 600 and 860 nm. These observations document that the parent absorption is preserved in the first anodic product, which can, therefore, be formulated as a half-oxidized dimer $[\mathbf{M4}\text{-}\mathbf{M4}]^{+}$. The **M4** component of the dimer becomes oxidized at a more positive anodic potential due to its interaction with $[\mathbf{M4}]^{+}$, probably via a π bonding between the central benzodithiophene moieties constituting the HOMO of parent **M4** (Figure S1). The existence of dimer $[\mathbf{M4}\text{-}\mathbf{M4}]^{+}$ also accounts for the splitting of the first anodic wave of **M4** at increasing concentration (> 10^{-5} M) into two waves exhibiting half peak currents compared to the first cathodic waves at -1.59 V and the anodic wave at 1.30 V. The latter probably corresponds to one-electron oxidation of monomer radical cation $[\mathbf{M4}]^{+}$ formed by rapid dissociation of transient $[\mathbf{M4}\text{-}\mathbf{M4}]^{2+}$ generated at 0.8 V. It needs to be appended that UV-vis-NIR spectroelectrochemistry with the OTTLE cell is insufficiently sensitive to monitor the direct oxidation of 10^{-5} M **M4** to the monomer radical cation indicated by DPV (Figure 2c) and thin-layer cyclic voltammetry. A detailed description of dimer $[\mathbf{M4}\text{-}\mathbf{M4}]^{+}$ with computational methods is out of scope of this work.

ChemComm Accepted Manuscript

View Article Online DOI: 10.1039/C6CC09184F

Published on 08 December 2016. Downloaded by University of Reading on 09/12/2016 09:02:42.

Considering the HOMO energy level and the slipped π-π stacking structure of **M6**, its application as an organic semiconductor was explored with field-effect transistor. Due to the strong self-assembly property, crystalline micro-/nano-sized structures were obtained instead of continuous thin films after a solution of **M6** had been deposited on a SiO_2 substrate. After careful optimization, the micro-/nano-sized wires were prepared through drop casting a solution of **M6** (CH_2Cl_2/petroleum ether 4:1, v/v) on an octadecyltrichlorosilane (OTS)-modified SiO_2 substrate. The micro-sized wire transistors were fabricated *in situ* as bottom-gate top-contact structure. The Au source and drain electrodes were fabricated through the "Au stripe mask" method.[22] More than ten devices were measured, all of them having displayed a characteristic p-channel behavior. The electrical characterization of **M6** revealed its good device performance with the mobility of 0.26 cm^2/Vs, that is one of the highest values measured for semiconductors based on FC-PACs.

To understand the measured field-effect mobility of **M6**, the morphology and packing structure of micro- / nano-sized wires were investigated through AFM and XRD. AFM images have shown that the wires have a rough surface with an RMS of 12.02 nm. The length of the wires ranged between several micrometers and several tens of micrometers, and the width was several micrometers. Surprisingly, the thickness of the wires was larger than two hundred nanometers. Wires with such a large thickness are rarely reported in organic transistors because of the large resistance between the source/drain electrodes and the conducting channel of transistor. The attempts to explore the stacking structure of **M6** in the wires with the selected area electron diffraction (SAED) technique failed.

Small-angle X-ray diffraction (XRD) has revealed that the wires are highly crystalline (Figure 4b). A series of peaks were observed at 4.46°, 8.90°, 13.33° and 17.82°, belonging to the set of *h00* diffractions according to the single crystal structure. The *d*-spacing estimated from the diffraction peaks is 19.895 Å. This value is very close to the *c*-axis length of compound **M6** (20.059 Å), indicating that **M6** has the *c* axis upright to the substrate in the micro-sized wires. With this orientation, the π-π stacking direction is parallel to the substrate surface according to the single crystal structure, which facilitates the transport of charge carriers.

In summary, a facile synthetic procedure yielding planar FC-PACs **M2**-**M6** has been developed. Single crystal diffraction results have revealed that **M2** forms dimers in the crystals, while slipped π-π stacking was observed in the crystal structure of **M6**. **M2 – M4** and **M6** exhibit rich redox chemistry, forming a semi-oxidized dimer with their radical cations at high solution concentrations. The micro-sized wire transistors of **M6** showed a good transistor performance with a hole mobility of 0.26 cm^2/Vs. All these results, together with a few reports on planar FC-PACs, have documented the potential of full-carbon five-membered aromatic ring-fused compounds for applications as functional materials.

This work was supported by the National Natural Sciences Foundation of China (Projects 21190031, 51273212) and the "Strategic Priority Research Program" of the Chinese Academy of Sciences (Project XDB12010100). FH thanks the University of Reading for the continued support of the Spectroelectrochemistry Reading laboratories (Project D14-015).

Notes and references

1 J. H. Dou, Y. Q. Zheng, Z. F. Yao, Z. A. Yu, T. Lei, X. X. Shen, X. Y. Luo, J. L. Sun, S.D. Zhang, Y. F. Ding, G. C. Han, Y. P. Yi, J. Y. Wang and J. Pei, *J. Am. Chem. Soc.,* 2015, **137**, 15947

2 N. J. Zhou, A. S. Dudnik, T. I. N. G. Li, E. F. Manley, T. J. Aldrich, P. J. Guo, H. C. Liao, Z. H. Chen, L. X. Chen, R. P. H. Chang, A. Facchetti, M. O. D. L. Cruz and T. J. Marks, *J. Am. Chem. Soc*., 2016, **138**, 1240

3 I. Yavuz, B. N. Martin, J. Y. Park and K. N. Houk, *J. Am. Chem. Soc.* 2015, **137**, 2856

4 P. M. Beaujuge and J. M. J. Frechet, *J. Am. Chem. Soc.* 2011, **133**, 20009

5 M. J. Kang, I. Doi, H. Mori, E. Miyazaki, K. Takimiya, M. Ikeda and H. Kuwabara, *Adv. Mater.*, 2011, **23**, 1222

6 C. Mitsui, J. Soeda, K. Miwa, H. Tsuji, J. Takeya and E. Nakamura, *J. Am. Chem. Soc.* 2012, **134**, 5448

7 C. Wetzel, E. Brier, A. Vogt, A. Mishra, E. M. Osteritz and P. Bauerle, *Angew. Chem. Int. Ed*. 2015, **54**, 12334

8 H. Xia, D. Q. Liu, X. M. Xu and Q. Miao *Chem. Commun.,* 2013, **49**, 4301

9 J. D. Wood, J. L. Jellison, A. D. Finke, L. C. Wang and K. N. Plunkett, *J. Am. Chem. Soc.* 2012, **134**, 15783

10 Z. U. Levi and T. Don Tilley. *J. Am. Chem. Soc.* 2010, **132**, 11012

11 G. E. Rudebusch, A. G. Fix, H. A. Henthorn, C. L. Vonnegut, L. N. Zakharov and M. M. Haley, *Chem. Sci*., 2014, **5**, 3627

12 D. T. Chase, A. G. Fix, S. J. Kang, B. D. Rose, C. D. Weber,Y. Zhong, L. N. Zakharov, M. C. Lonergan, C. Nuckolls and M. M. Haley, *J. Am. Chem. Soc.* 2012, **134**, 10349

13 M. F. Wang, A. R. Mohebbi, Y. M. Sun and F. Wudl, *Angew. Chem. Int. Ed.* 2012, **51**, 6920

14 H. Y. Li, F. S. Kim, G. Q. Ren, E. C. Hollenbeck, S. Subramaniyan and S. A. Jenekhe, *Angew. Chem*. *Int. Ed.* 2013, **125**, 5623

15 X. Gu, X. M. Xu, H. Y. Li, Z. F. Liu and Q. Miao, *J. Am. Chem. Soc.*, 2015, **137**, 16203

16 A. C. Fahrenbach, J. C. Barnes, D. A. Lanfranchi, H. Li, A. Coskun, J. J. Gassensmith, Z. Liu, D. Benitez, A. Trabolsi, W. A. Goddard, M. Elhabiri and J. F. Stoddart, *J. Am. Chem. Soc.* 2012, **134**, 3061

17 H. Zhylitskaya, J. Cybinska, P. Chmielewski, T. Lis and M. Stepien, *J. Am. Chem. Soc.* 2016, DOI: 10.1021/jacs.6b07826

18 C. C. Ferron, M. Capdevila-Cortada, R. Balster, F. Hartl, W. Niu, M. He, J. J. Novoa, J. T. Lopez Navarrete, V. Hernandez and M. C. Ruiz Delgado, *Chem. Eur. J.* 2014, **20**, 10351.

19 When non-substituted benzo[1,2-*b*:4,5-*b'*]- dithiophene was used, an insoluble product was obtained. Its high resolution mass spectrum nevertheless proved the successful synthesis of the corresponding FC-PAC.

20 C. C. Ferron. M. C. Ruiz Delgado, V. Hernandez, J. T. Lopez Navarrete, B. Vercelli, G. Zotti, M. C. Cortada, J. J. Novoa, W. Niu, M. He and F. Hartl, *Chem. Commun.* 2011, **47**, 12622

21 The second reduction potential -1.9 V is very close to the end of the cathodic potential window of CH_2Cl_2, which prevented the measurement of the electronic absorption spectrum of stable $[\mathbf{M4}]^{2-}$ at this electrode potential.

22 Y. Xiong, J. Tao, R. Wang, X. Lan, X. Yang, D. Wang, H. Wu and H. Li, *Adv. Mater.*, 2016, **28**, 5949.

ChemComm Accepted Manuscript

 This journal is © The Royal Society of Chemistry 20xx